Journal of Marine Science and Technology

Volume 31 | Issue 1 Article 5

Influence Of Vacuum Condition On Rapid Chloride Migration (Rcm) Test For Chloride Penetration Resistance Of Concrete

Chih-Yen Lin
Department of Harbor and River Engineering, National Taiwan Ocean University, 2 Pei-Ning Road, Keelung 20224, Taiwan, 21052005@mail.ntou.edu.tw

Chun-Fu Chang
Department of Harbor and River Engineering, National Taiwan Ocean University, 2 Pei-Ning Road, Keelung 20224, Taiwan

Chung-Chia Yang
Department of Harbor and River Engineering, National Taiwan Ocean University, 2 Pei-Ning Road, Keelung 20224, Taiwan, ccyang@mail.ntou.edu.tw

Recommended Citation

Lin, Chih-Yen; Chang, Chun-Fu; and Yang, Chung-Chia (2023) "Influence Of Vacuum Condition On Rapid Chloride Migration (Rcm) Test For Chloride Penetration Resistance Of Concrete," *Journal of Marine Science and Technology*: Vol. 31: Iss. 1, Article 5.
DOI: 10.51400/2709-6998.2684
Available at: https://jmstt.ntou.edu.tw/journal/vol31/iss1/5

RESEARCH ARTICLE

Influence of Vacuum Condition on Rapid Chloride Migration (RCM) Test for Chloride Penetration Resistance of Concrete

Chih-Yen Lin, Chun-Fu Chang, Chung-Chia Yang*

Department of Harbor and River Engineering, National Taiwan Ocean University, 2 Pei-Ning Road, Keelung 20224, Taiwan

Abstract

NT Build 492 regulates that the pressure be set at 7.5−37.5 torr and be maintained for 3 h for vacuum processing. This large range of acceptable vacuum pressure is awkward for research, and 3 h of pump-down time may be excessive. In this study, vacuum conditions were divided into vacuum pressure and pump-down time groups: various vacuum pressures and pump-down times were used to preprocess specimens to explore the effect of vacuum conditions on the RCM test. The salt ponding test was also conducted to identify the optimal vacuum conditions. It is shown that the relationship between vacuum pressure and the migration coefficient approximates an exponential function with vacuum pressure group. Moreover, the vacuum pressure should be lower than 7.5 torr to obtain accurate results from RCM test. For pump-down time group, using a vacuum pressure of 2 torr can shorten the pump-down time to 1 hour and improve the test efficiency; vacuum pressures of 30 torr should not be used. Finally, this study indicates the most suitable vacuum conditions for RCM test by establishing relationship between diffusion and migration coefficients: 1−2 torr of vacuum pressure and 1 hour of pump-down time.

Keywords: Rapid Chloride Migration test, Vacuum condition, Salt ponding test

1. Introduction

The migration coefficient of concrete can be used as a basis for evaluating the service life of structures and is thus a key quality control index. Coastal structures are affected by chloride ions carried on sea breezes. Chloride ions diffuse through the pores and invade into concrete through capillary action, ion diffusion, and osmosis in solution [4,5,15]. Chloride ions diffusing into the surface of steel bars accelerate corrosion [6,24] and can cause tensile failure in concrete [12,21]. Thus, resistance to the effects of chloride ions is a key indicator of concrete durability.

The rapid chloride migration (RCM) test involves an electrochemical test, colorimetry [8], and the calculation of the non-steady-state migration coefficient [10]. RCM is a critical test for evaluating concrete durability and has been used in numerous studies. Hesong et al. used proportions of 15%, 30%, and 60% ground granulated blast-furnace slag (GGBFS) to replace cement in concrete specimens. They explored the effect of GGBFS on the durability and porosity of concrete by applying the RCM test, mercury intrusion porosimetry, and scanning electron microscopy. The results revealed that GGBFS can reduce the capillary porosity of concrete and improve the resistance of concrete to erosion by harmful ions [13]. Liu et al. conducted RCM tests on concrete containing fly ash and reported that including fly ash can substantially improve the durability of concrete [14]. Emanuele et al. conducted RCM tests on the specimens containing healing agents and reported that the healing agents

Received 1 June 2022; revised 15 December 2022; accepted 12 January 2022.
Available online 31 March 2023

* Corresponding author.
E-mail address: ccyang@mail.ntou.edu.tw (C.-C. Yang).

https://doi.org/10.51400/2709-6998.2684

could form dense calcium carbonate to fill the cracks in the specimens. However, the effect was limited because cracks filled with calcium carbonate were still the lowest barrier to the primary path for ion migration. Accordingly, calcium carbonate cannot effectively improve the durability of concrete [19]. Clay et al. conducted RCM tests to assess the chloride migration characteristics and reliability of reinforced concrete highway structures in Pennsylvania, United States. Specifically, 68 concrete samples with different ratios of mineral admixture and aggregate were used for the RCM test. The test results were organized through reliability analysis, and a mathematical model was established based on Fick's Second Law [16]. Clay et al. reported that reinforced concrete in highway structures had a 10% chance of corroding within 15 years [16]. Shiu and Yang [20] used the chloride profile established after RCM tests to determine the migration coefficient, the migration coefficient, which was obtained from RCM test, correlates linearly with the migration coefficient, obtained from the chloride profile. These studies reveal that the RCM test has been applied and discussed by numerous researchers, has satisfactory experimental accuracy, and is efficient for practical applications. The RCM test was standardized in Northern Europe as NT Build 492 [17] in 1999 and in the United States as AASHTO-T357 [3] in 2019, further indicating the importance of RCM test.

In the RCM test, the migration of chloride ions into concrete is accelerated by an external electric field to reduce the excessive time required for the diffusion of chloride ions in the salt ponding test, increasing testing efficiency. However, compared with the salt ponding test, RCM tests are subject to additional variables such as the vacuum condition, the applied voltage, test time of chloride migration, and the concentration of the colorimetric color boundary. These variables can reduce the reliability of durability evaluation with the RCM test. Spiesz and Brouwers applied different voltages to perform RCM test. Applying different voltages did not affect the migration coefficient [22]. Spiesz and Brouwers discovered that, after vacuum preprocessing, the porosity of the specimen was not unsaturated; they suggested that this phenomenon required further exploration [22]. Chiang used water immersion, boiling, and vacuum to pretreating specimens in rapid chloride permeability test (RCPT) to investigate the saturation level of specimens caused by various treatments as indicated by electric power usage [7]. The research revealed that the boiling treatment required the greatest electric power, followed by vacuum and immersion. The water immersion and boiling treatments thus produced specimens with the lowest and highest saturation, respectively. However, the boiling treatment accelerated the hydration of the specimens and affected their material properties. Therefore, vacuum preprocessing is a critical step in the RCM test.

NT Build 492 [17] regulates that the pressure be set at 7.5−37.5 torr and be maintained for 3 h for vacuum processing. This large range of acceptable vacuum pressure is awkward for research and may result in testing errors or misinterpretations of concrete durability. Moreover, 3 h of pump-down time may be excessive; reducing the pump-down time could substantially improve the testing efficiency. In this study, various vacuum pressures and pump-down times were used to preprocess specimens to explore the effect of vacuum conditions on the RCM test. The salt ponding test was also conducted to identify the optimal vacuum conditions.

2. Experimental program

In this study, RCM test and salt ponding test were performed. Vacuum preprocessing parameters were the main experimental variables, and vacuum conditions were divided into vacuum pressure and pump-down time groups. In the salt ponding test, layer-by-layer grinding and the two-plate method were adopted to sample the depth of the specimens. Fig. 1 presents a flow chart of the experiment.

2.1. Concrete mix design and specimen preparation

In this study, concrete with water−cement ratios of 0.35, 0.45, 0.55, or 0.65 (C3, C4, C5, and C6, respectively) were used. To reduce the number of testing variables, the volume of coarse and fine aggregates was fixed (coarse aggregates 35%, fine aggregates 30%). Water-reducing agents accounted for 0.65% and 0.3% of the cement weight for the specimens with a water−cement ratio of 0.35 and 0.45, respectively. The concrete mixes are listed in Table 1. Cylindrical specimens with a diameter of 10 cm and a height of 20 cm were prepared and were cured in water for 28 days. A wet cutter was used to cut the specimens of RCM test into pieces with a diameter of 10 cm and a height of 5 cm and to cut the salt ponding test specimens into pieces with a diameter of 10 cm and a height of 10 cm.

2.2. Vacuum preprocessing

Fig. 2 displays the vacuum equipment used in this study. The vacuum pump and specimen chamber are presented on the left and right sides of Fig. 2, respectively. While the vacuum pump is on, the

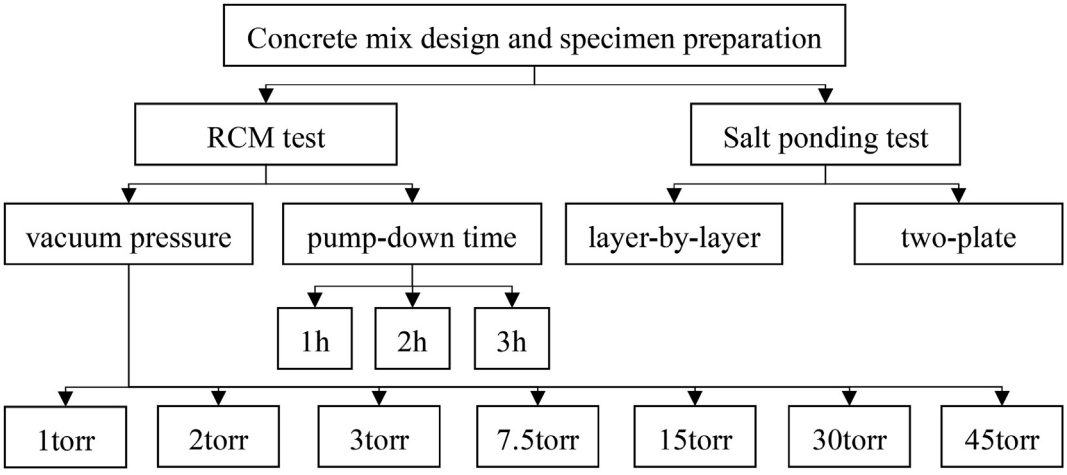

Fig. 1. The flow chart of the experiment.

Table 1. Concrete mix design.

Mix	W/C	Unit: kg/m^3				
		Water	Cement	C.A.	F.A.	SP
C3	0.35	170	495	928	774	3.2
C4	0.45	192	430	928	774	1.3
C5	0.55	209	380	928	774	0
C6	0.65	222	341	928	774	0

pressure of the specimen chamber continues to drop and pressure cannot be maintained. Therefore, the time and vacuum pressure values were recorded in this study during the vacuum process, as shown in Fig. 3 (a). Trapezoidal rule of the time and vacuum pressure values was performed, as presented in Fig. 3 (b). The area below the vacuum−pressure−time curve is displayed in Fig. 3 (c). The mean vacuum pressure was calculated by dividing the total area under the curve by the time, as shown in Fig. 3 (d). The vacuum pump was controlled during the actual pumping pressure to approximate the target value. When the vacuum conditions were controlled, saturated calcium hydroxide solution was added to the airtight specimen chamber until the specimens were submerged, and 1 hour of wet pumping was performed. Then, the specimens were

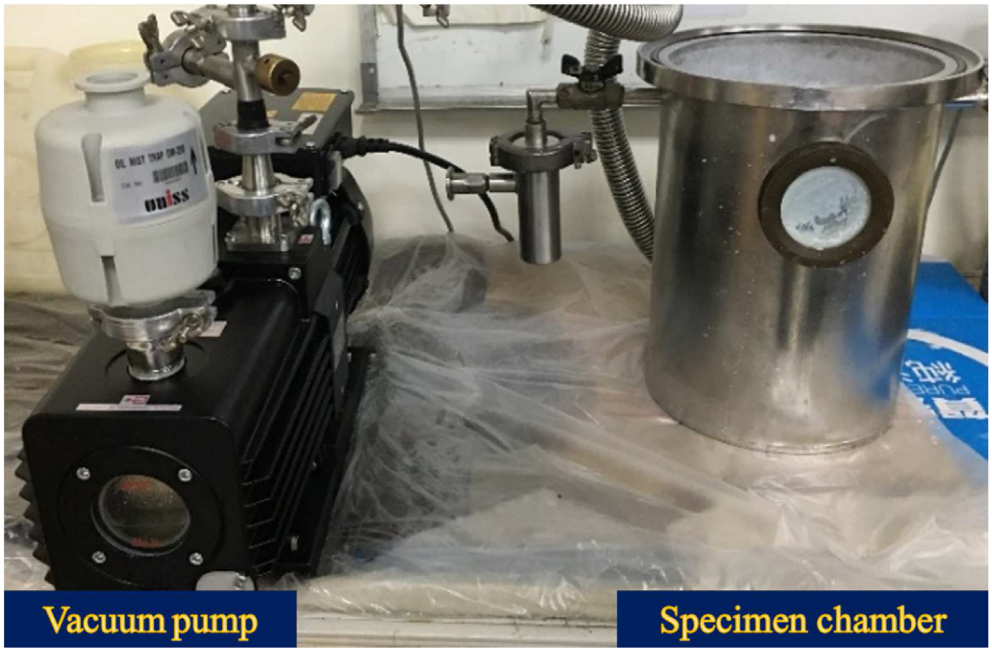

Fig. 2. Vacuum equipment.

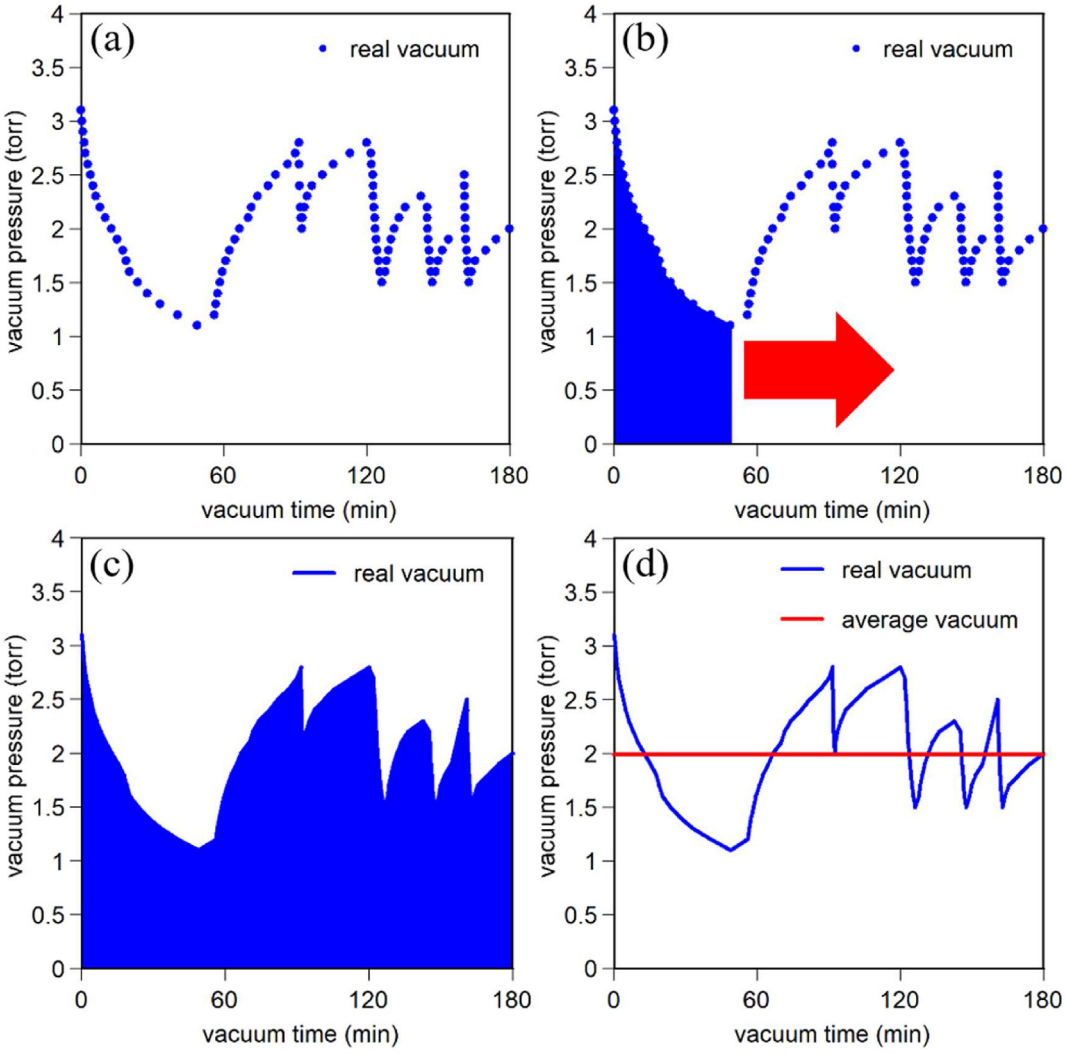

Fig. 3. Vacuum time correspond to vacuum pressure during the vacuum process: (a) Vacuum time correspond to vacuum pressure; (b) Trapezoidal rule of the time and vacuum pressure; (c) The area of vacuum pressure-time; (d) Real vacuum and average vacuum.

immersed in saturated calcium hydroxide solution for approximately 18 hours.

2.3. Migration test and non-steady-state migration coefficient

The preprocessed specimens were placed into the electrical equipment; the anode was 350 mL of 0.3 M NaOH solution and the cathode was 7 L of 10% NaCl solution, as presented in Fig. 4 (a). Migration test was thus completed in accordance with the specified electrification conditions by standard. After electrification, the specimens were split axially with a compression machine, and 0.1 N silver nitrate was evenly sprayed on the split surface. After chloride ions reacted with silver nitrate to form a white precipitate, the penetration depth was measured. The measurement method, presented in Fig. 4 (b), is described as follows: The chloride penetration depth x_d was calculated by averaging the values of seven points measured in the middle of the sample; the outermost 1 cm on each side was excluded from the measurement. The test parameters such as voltage, duration, and penetration depth were substituted into Equation (1) to calculate the non-steady-state migration coefficient (M):

$$M = \frac{0.0239(273+T)L}{Ut}\left(x_d - 0.0238\sqrt{\frac{(273+T)x_d L}{U}}\right). \quad (1)$$

In Equation (1), M is the migration coefficient (10^{-12} m^2/s), U is the applied voltage (V), T is the temperature (°C), L is the thickness of the specimen

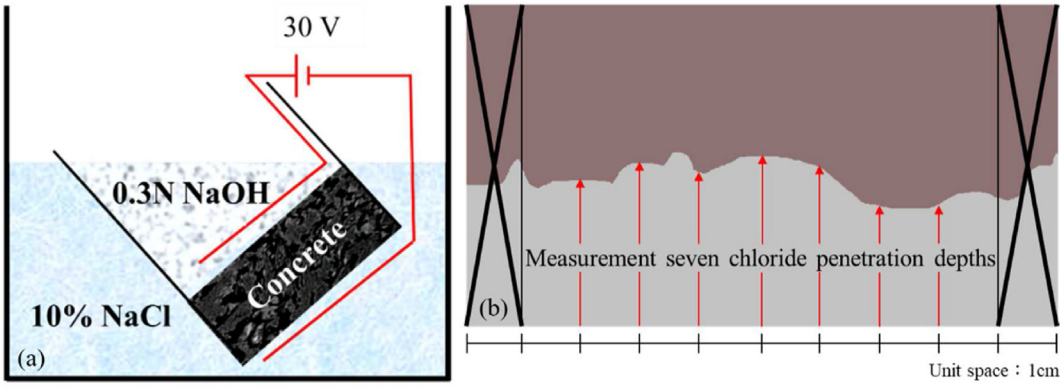

Fig. 4. (a) Migration test equipment; (b) The measurement method of penetration depths.

(mm), x_d is the penetration depths (mm), t is the test duration (hour).

2.4. Salt ponding test

Concrete with water–cement ratios of 0.35, 0.45, 0.55, and 0.65 (Table 1) were used for the salt ponding test. The specimens were coded using P (ponding). The diffusion coefficient of each concrete mix was averaged from the diffusion coefficients of three specimens. The salt ponding test was conducted by in accordance with AASHTO T259 [1]; thus, 3% saline was poured into the cofferdam (top of the specimens) and the specimens were soaked for 91 days (Fig. 5). Depth sampling for each concrete mix was performed by layer-by-layer grinding for one specimen and the two-plate method was used for two specimens.

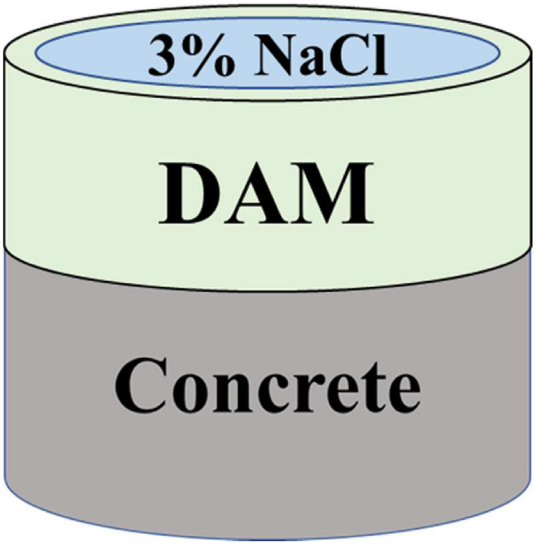

Fig. 5. Salt ponding test.

2.4.1. Layer-by-layer grinding

The specimens were ground and sampled layer-by-layer at 6 depths. The first four layers were sampled with a grinding–boring machine and had thickness of 0.3 cm. The fifth and sixth layers were sliced for sampling at a depth of 2.5 cm and 3–4 cm, respectively. The samples were ground into powder with a pulverizer. After sampling, the chloride content of each sample was analyzed in accordance with AASHTO T260 [2], and a sample depth–chloride content diagram was produced.

2.4.2. Two-plate method

The two-plate method was conducted according to the suggestions in Huang and Yang [11]. Huang and Yang deduced that the chloride profile can be expressed as Equation (2) [11]:

$$C = C_s \times exp\left(-\frac{\pi C_s^{\,2}}{4m^2}x^2\right). \quad (2)$$

In Equation (2), C is the chloride content (%), C_s is the chloride content on the surface (%), x is depth of diffused (cm), and m is the total chloride content (%).

According to Equation (2), the C_s and m are the crucial parameters of the chloride profile. To measure C_s, the first 0.3-cm-think layer (the surface) was sampled with a grinding-boring machine. The second layer was sliced for sampling at a depth of 3–4 cm. All the chloride in the slices were included in the sampled powder. The two-plate sampling method was used to obtain the first-layer chloride content (C_1) at a sampling depth of L_1 and the second-layer chloride content (C_2) at a sampling depth of L_2. Equation (3) was used to calculate the total chloride content (m):

$$m = C_1L_1 + C_2L_2. \quad (3)$$

Table 2. The actual vacuum pressure in the vacuum pressure group.

Mix	Target vacuum in pump-down time 3 hours (torr)						
	1	2	3	7.5	15	30	45
C3	0.97	1.99	3.00	7.52	15.55	30.51	44.96
C4	0.98	2.00	2.99	7.47	15.35	30.72	44.53
C5	0.98	2.00	2.99	7.47	15.35	30.72	44.53
C6	0.97	1.99	3.00	7.52	15.55	30.51	44.96

Note: The unit of actual vacuum pressure is torr.

To obtain C, m and C_s *are* substituted into Equation (2), and C_s was calculated by trial and error.

3. Results and discussion

The effects of different vacuum pressures and pump-down times on the non-steady-state migration coefficient were investigated. The diffusion coefficient used to identify the optimal vacuum conditions was discussed.

3.1. Vacuum conditions

During the vacuum pretreatment of the specimens, the system was controlled by turning on and off the vacuum pump. The vacuum pressure for the specimens in the vacuum pressure group and in the pump-down time group are listed in Table 2 and Table 3, respectively. For all specimens, the difference between the actual and target vacuum pressures was below 3%, indicating that the vacuum conditions were well-controlled.

3.2. Initial current in the RCM tests

The preprocessed specimens were assembled with the electric equipment according to Fig. 4 (a) In accordance with NT Build 492 [17], the initial current (I_{30}) was measured when the equipment was energized at 30 V. In Fig. 6, the x- and y-axes denote the vacuum pressure and initial current, respectively, and the initial current corresponding to each vacuum pressure was averaged from three currents. For specimens of different water−cement ratios, an increase in the initial current was correlated with a decrease in the vacuum pressure, implying that increased evacuation causes a reduction in the saturation of the porosity in specimens, resulting in a higher current when the equipment was energized.

Table 3. The actual vacuum pressure in the pump-down time group.

Actual vacuum (torr)						
Pump-down time (h)	1	1	2	2	3	3
Target vacuum (torr)	2.00	30.00	2.00	30.00	2.00	30.00
C3	2.02	29.13	2.02	29.41	2.01	29.90
C4	1.99	29.89	2.00	29.96	2.00	30.03
C5	1.99	29.89	2.00	29.96	2.00	30.03
C6	2.02	29.13	2.02	29.41	2.01	29.90

The initial currents for C3 and C6 were 76.5 mA and 155.5 mA, respectively. Initial currents increased as the water−cement ratio of the specimens increased. The voltage of migration test was determined according to the initial current data in Fig. 6. Voltages of 25, 20, 15, and 10 V were applied to C3, C4, C5, and C6, respectively, for 24 hours. Chloride at the negative electrode were rapidly migrated into the concrete specimens due to the electric field.

3.3. Effect of vacuum pressure on the RCM test

Following migration test, specimens were split axially with a compression machine, and 0.1 N silver nitrate was sprayed on the split surface. Silver ions undergo photochemical reactions with chloride ions and with hydroxide ions [18], presented in Equations (4) and (5), which result in white and brown precipitates, respectively (Fig. 7). Fig. 7 displays colorimetric photos of C6 specimens with various vacuum pressures; the red line indicates the mean penetration depth of the chloride. The penetration depth of chloride increased significantly with the decrease in vacuum pressure. A 25% difference was observed between the penetration depth of the chloride at a vacuum pressure of 1 torr and 45 torr. The chloride penetration depth, voltage, duration, and other parameters were substituted into Equation (1) to calculate the migration coefficient; the data are listed in Table 4.

$$Ag^{+} + Cl^{-} \rightarrow AgCl\downarrow (silver\ white) \tag{4}$$

$$2Ag^{+} + 2OH^{-} \rightarrow 2AgOH \rightarrow H_2O + Ag_2O\downarrow (brown) \tag{5}$$

The mean migration coefficient of C3 obtained under a vacuum pressure of 1 torr and 45 torr differed by 3.5 (10^{-8} cm^2/s); those of C6 differed by 7.7 (10^{-8} cm^2/s). As the vacuum pressure increased, the migration coefficient was decreased less in specimens with higher a water−cement ratio. Fig. 8 (a) and (b) present the migration coefficient for C3 and C6, respectively; the x-axis indicates vacuum pressure and the y-axis indicates the migration coefficient. Curve fitting for Fig. 8 (a) and (b) revealed that the relationship between vacuum pressure and the migration coefficient approximates an exponential

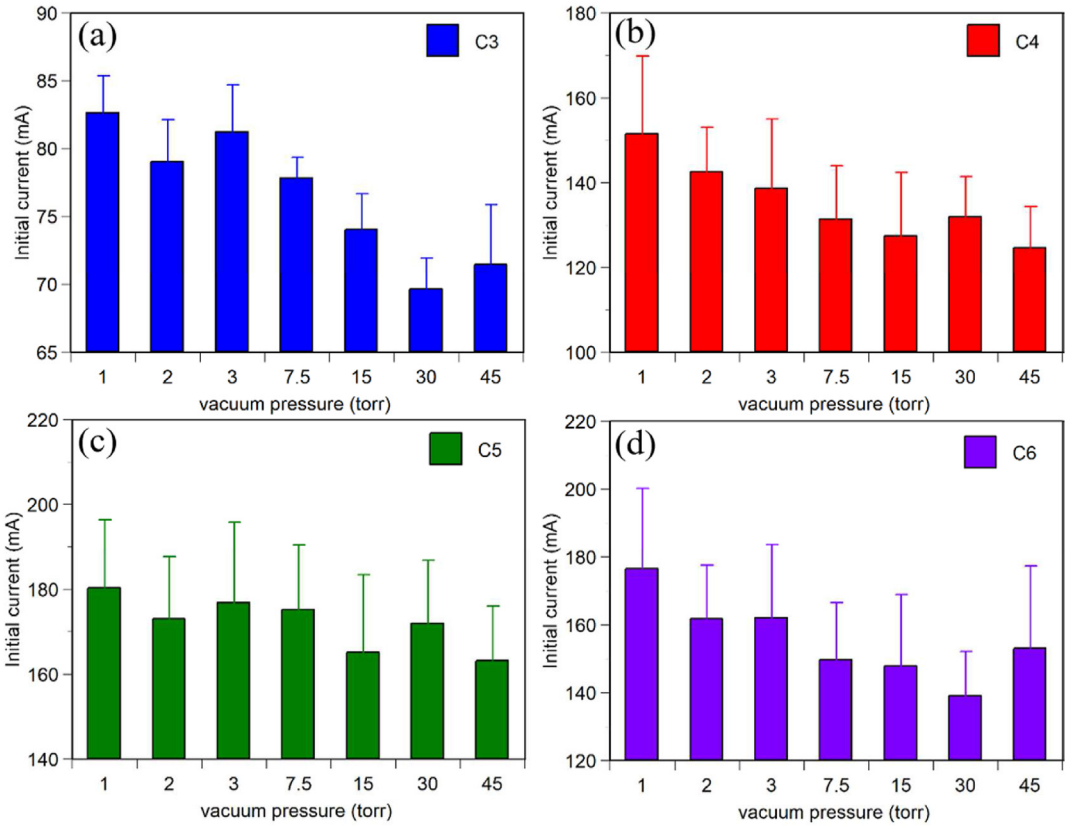

Fig. 6. The vacuum pressure vs. the initial current: (a) 0.35 W/C (C3); (b) 0.45 W/C (C4); (c) 0.55 W/C (C5); (d) 0.65 W/C (C6).

function. The migration coefficient decreased as the increase in vacuum pressure, implying a decrease in the saturation of specimens. For vacuum pressures of 1−7.5 torr, the migration coefficient approximated the fitting curve; for vacuum pressures of 15−45 torr, the migration coefficient deviated from the fitting curve. Thus, the vacuum pressure should be lower than 7.5 torr to obtain accurate migration coefficient.

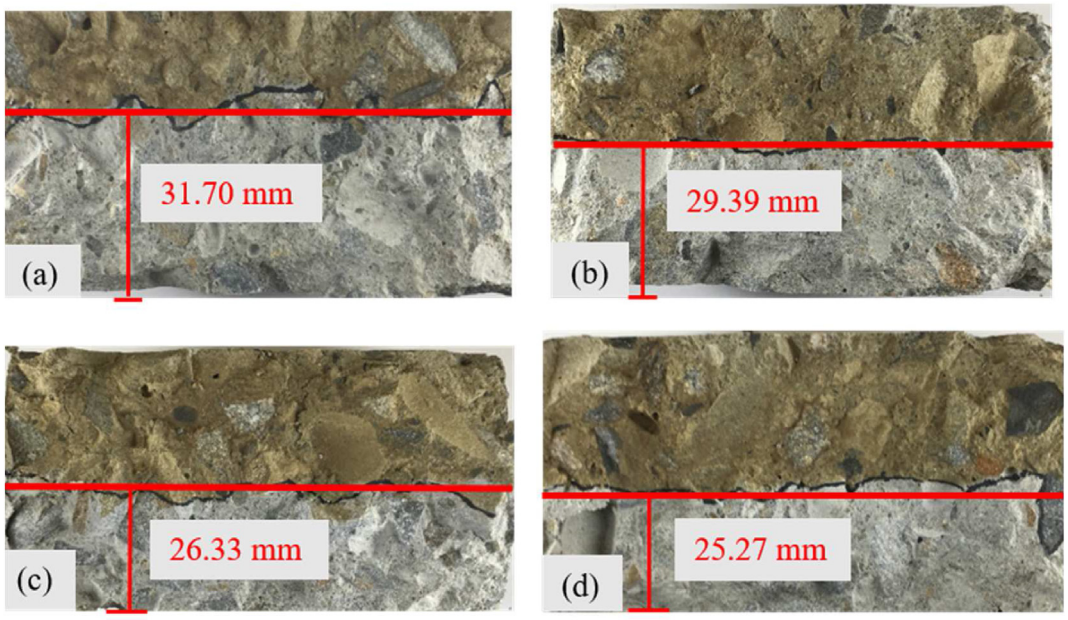

Fig. 7. Colorimetric photos of C6 specimens with various vacuum pressures: (a)1 torr; (b)3 torr; (c)15 torr; (d)45 torr.

Table 4. The migration coefficient in the vacuum pressure group.

Migration coefficient (10^{-8} cm^2/s)								
Mix	Test number	Vacuum pressure (torr)						
		1.0	2.0	3.0	7.5	15.0	30.0	45.0
C3	1	13.8	13.0	13.2	12.2	11.9	11.1	10.2
	2	14.6	12.9	12.7	12.9	12.1	10.5	11.5
	3	14.0	13.0	12.8	12.2	11.7	11.6	10.1
	average	14.1	13.0	12.9	12.4	11.9	11.1	10.6
C4	1	27.1	25.1	23.9	23.1	21.6	21.9	21.5
	2	26.4	24.8	23.1	22.1	21.3	20.6	23.2
	3	25.4	23.5	24.9	22.2	22.9	20.7	20.4
	average	26.3	24.5	24.0	22.5	21.9	21.1	21.7
C5	1	36.5	35.0	35.1	34.1	34.5	31.7	31.8
	2	36.8	35.4	35.8	33.2	33.6	33.2	33.4
	3	36.3	35.7	34.9	33.3	33.6	32.6	32.7
	average	36.5	35.4	35.3	33.5	33.9	32.5	32.6
C6	1	40.5	38.8	37.3	34.3	35.0	32.0	31.4
	2	39.5	39.3	37.9	35.1	34.1	32.3	32.9
	3	40.9	39.9	37.9	34.2	32.9	34.4	34.2
	average	40.2	39.3	37.7	34.5	34.0	32.9	32.8

3.4. Effects of pump-down time on the RCM test

Fig. 9 displays the colorimetric photos of C3 specimens with a vacuum pressure of 2 torr with different pump-down times. For pump-down times from 1 to 3 hours, the penetration depth of chloride did not differ substantially (0.46%).

Fig. 10 presents the migration coefficient conducted with different pump-down time; the x-axis indicates pump-down time and the y-axis indicates the migration coefficient. Fig. 10 (a) and (b) present the migration coefficient for vacuum pressures of 2 and 30 torr, respectively. Fig. 10 (a) reveals that the maximum errors of the migration coefficient for specimens C3, C4, C5, and C6 with a vacuum pressure of 2 torr and pump-down times of 1, 2, or 3 h were 3.37%, 4.80%, 2.73%, and 0.88%, respectively—all below 5%. As presented in Fig. 10 (b), the maximum errors of the migration coefficient of specimens C3, C4, C5, and C6 under a vacuum pressure of 30 torr and a pump-down time of 1, 2, or 3 h were 1.31%, 1.81%, 6.76%, and 9.65%, respectively. Accordingly, the error of the migration coefficient at a vacuum pressure of 30 torr was large for specimens C5 and C6. These errors reveal that, for a vacuum pressure of 2 torr, pump-down times of 1−3 h do not substantially affect the migration coefficient. For a vacuum pressure of 30 torr, pump-down time changes did not affect the migration coefficient of specimens with a low water−cement ratio (C3, C4), but had a greater effect for specimens with a high water−cement ratio (C5, C6).

To further explore the effect of pump-down time on the migration coefficient, the coefficient of variation (CV) of the migration coefficient was calculated for different pump-down times (Table 5); these were no more than 2% for a vacuum pressure of 2 torr and reached 2.68% and 3.76% for C5 and C6, respectively, at vacuum pressures of 30 torr (Table 5). A greater CV value for the migration coefficient was obtained for specimens with higher water−cement ratios (C5, C6) under a vacuum pressure of 30 torr. The insufficient evacuation under a vacuum pressure of 30 torr resulted in uneven porous saturation of specimens, which was affected by the pump-down time. Thus, using a vacuum pressure of 2 torr can shorten the pump-down time to 1 hour and improve the test efficiency; vacuum pressures of 30 torr should not be used.

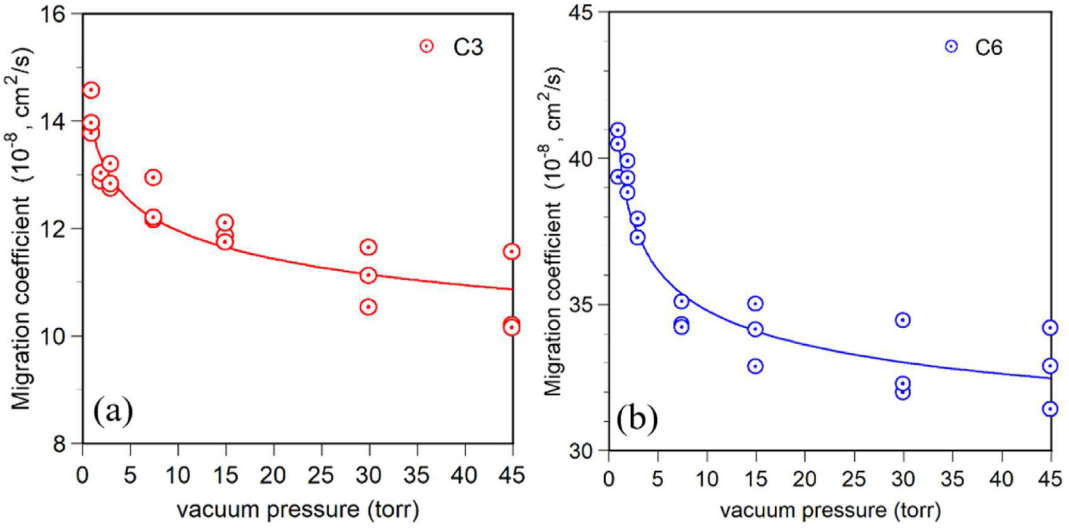

Fig. 8. The vacuum pressure vs. migration coefficient: (a) 0.35 W/C (C3); (b) 0.65 W/C (C6).

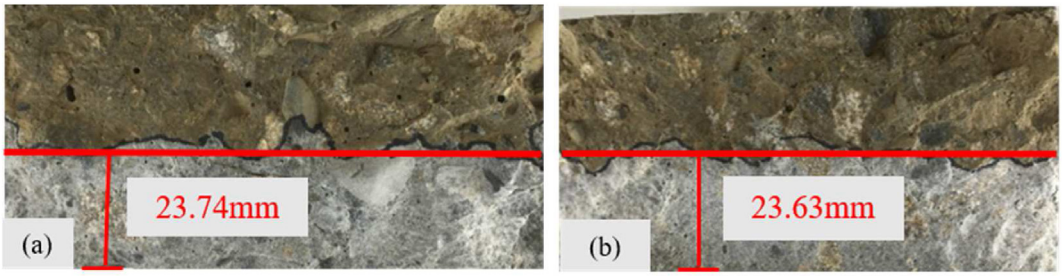

Fig. 9. Colorimetric photos of C3 specimens with various pump-down time: (a) pump-down 1h; (b) pump-down 3h.

3.5. Diffusion coefficient

In the salt ponding test, chloride enter the concrete specimens through diffusion and capillary action. The diffusion phenomenon in the salt ponding test can be expressed as Equation (6), a mathematical equation based on Fick's Second Law:

$$\frac{\partial C}{\partial t} = D\frac{\partial^2 C}{\partial x^2}. \quad (6)$$

In Equation (6), C is the chloride content (%), t is the duration of test (s), x represents the diffusion depth (cm), and D denotes the diffusion coefficient (cm^2/s).

Fick's Second Law describes time-dependent concentration gradients and diffusion flux at a certain depth. Crank [9] set the boundary conditions ($C = C_s$, $x = 0$, $t > 0$; $C = 0$, $x > 0$, $t = 0$) and solved the partial differential equation of Equation (6) to obtain an explicit solution.

$$C = C_s \times exp\left(\frac{-x^2}{2Dt}\right). \quad (7)$$

In Equation (7), C is the chloride content (%), C_s is the chloride content on the surface (%), x represents the depth of diffused, t is duration of test (s).

Table 5. The coefficient of variation (CV) of the migration coefficient with various pump-down times.

Mix	Vacuum pressure (torr)	Migration coefficient (10^{-8} cm^2/s)			CV (%)
		1h	2h	3h	
C3	2	12.56	12.15	12.47	1.42
C4		23.73	24.61	24.87	2.00
C5		35.14	35.15	36.10	1.27
C6		38.85	38.79	38.51	0.38
C3	30	11.61	11.51	11.46	0.54
C4		21.32	20.94	21.02	0.78
C5		31.79	33.94	32.74	2.68
C6		38.96	37.45	35.53	3.76

Note: The CV is the coefficient of variation.

The two-plate chloride profile proposed by Huang and Yang [11], Equation (2), was derived from Equation (7). The two are equivalent, and Equation (8) can be obtained by manipulating the terms of Equations (2) and (7):

$$D = \frac{2m^2}{\pi C_s{}^2 t}. \quad (8)$$

The salt ponding test was performed to obtain chloride content corresponding to the depth of sampled specimens, as illustrated by Fig. 11, in which the x-axis is the depth of specimen and the y-

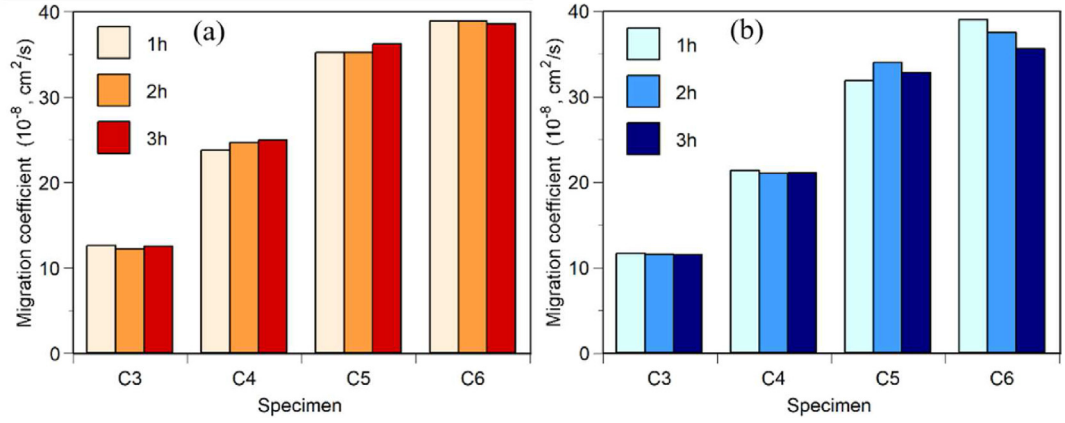

Fig. 10. The migration coefficient with various pump-down time: (a) 2 torr; (b) 30 torr.

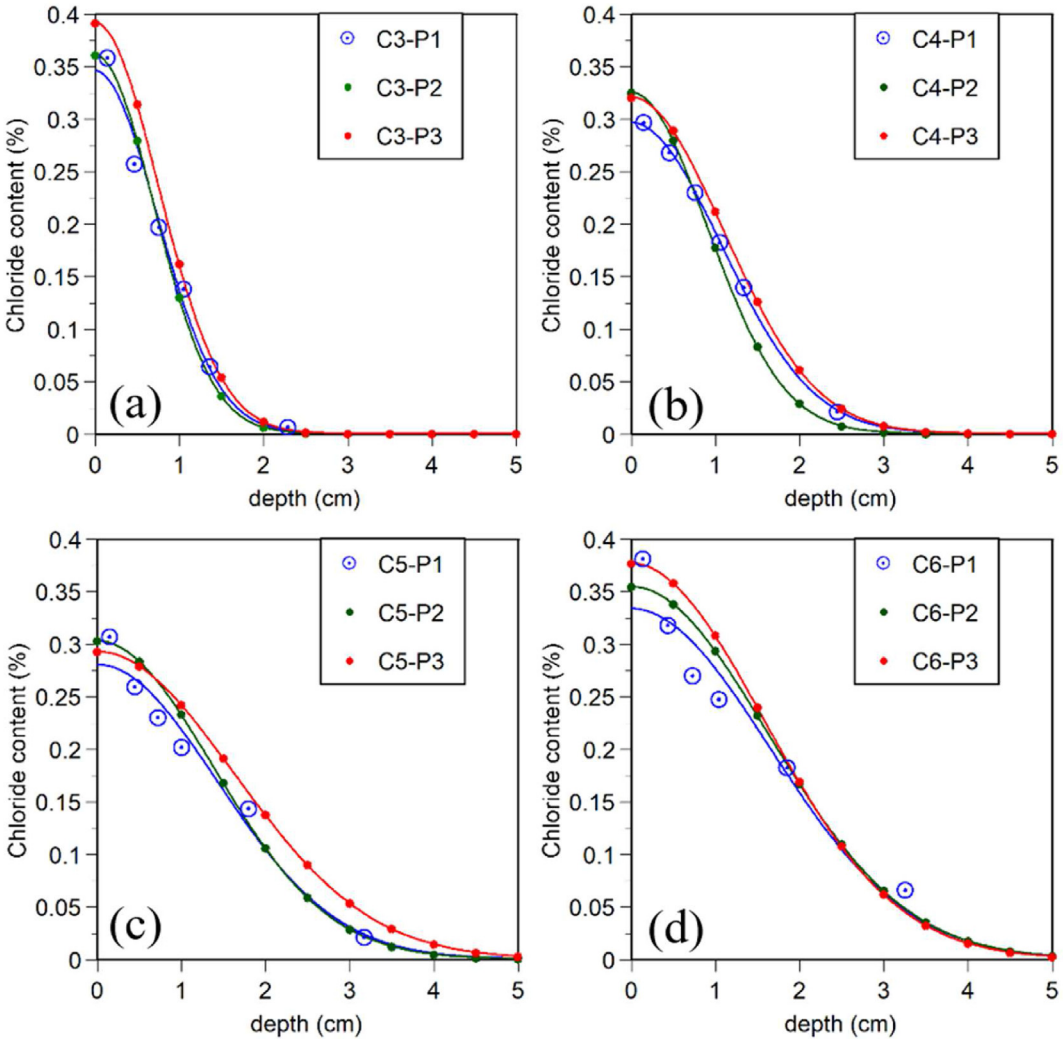

Fig. 11. The chloride profiles: (a) 0.35 W/C; (b) 0.45 W/C; (c) 0.55 W/C; (d) 0.65 W/C.

axis is the chloride content. Layer-by-layer grinding was applied for P1, whereas the two-plate method was applied for P2 and P3 (Fig. 11). Equation (7) for P1 were used for curve fitting to obtain the diffusion coefficient (D). The distribution curve of the chloride contents for P2 and P3 was fit based on Equation (2), and the diffusion coefficient (D) was calculated using Equation (8). As presented in Fig. 11, the distribution curves of the chloride content treated with layer-by-layer grinding and the two-plate method were in good agreement. The diffusion coefficients of all specimens are listed in Table 6, which reveals that increases in the water−cement ratio result in deeper chloride diffused depth and a greater diffusion coefficient. The durability of the specimens decreased as the water−cement ratio increased.

Table 6. Diffusion coefficient of all specimen.

Mix	Diffusion coefficient (10^{-8} cm^2/s)			
	P1	P2	P3	average
C3	6.94	6.22	7.21	6.79
C4	14.89	10.52	15.35	13.59
C5	26.04	24.26	33.68	27.99
C6	34.57	33.83	31.73	33.38

3.6. Relationship between diffusion and migration coefficients

The durability of concrete can be measured with both the diffusion and migration coefficients, which are calculated through traditional diffusion test and accelerated ion migration with an external electric field, respectively. Thus, these coefficients are related to a certain extent. The diffusion coefficient closely resembles diffusion behavior in real-world structures, whereas the migration coefficient can be

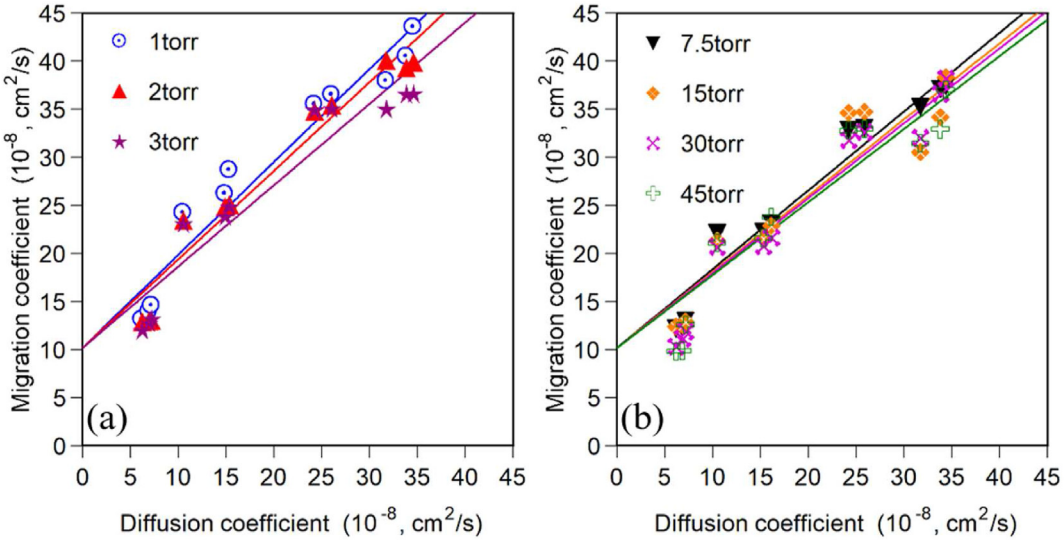

Fig. 12. The relationship between migration coefficient and diffusion coefficient in the vacuum pressure group: (a)1, 2, 3 torr; (b)7.5, 15, 30, 45 torr.

affected by experimental variables such as the vacuum, electric field, and differences in discoloration. The diffusion coefficient were used as the basis to evaluate the migration coefficient in this study. Figs. 12 and 13 present the linear relationship between the diffusion and migration coefficients; this relationship can be expressed with Equation (9):

$$M = a \times D + b. \tag{9}$$

In Equation (9), M is the migration coefficient (10^{-8} cm^2/s); a is the slope; D is the diffusion coefficient (10^{-8} cm^2/s); and b is the experimental constant. Because the migration coefficient is composed of two elements: diffusion and electromigration [23], Yang et al. [25] indicated that the migration coefficient is higher than the diffusion coefficient. Based on the experimental data (Figs. 12 and 13), the regression analysis showed that the experimental constants (b) are proximity 10^{-7} (cm^2/s) in all specimens.

Fig. 12 presents the relationship between the migration and diffusion coefficients at various vacuum pressures. The slopes for 1, 2, and 3 torr are 0.96, 0.92, and 0.84, respectively [Fig. 12 (a)], and those for 7.5, 15, 30, and 45 torr are 0.83, 0.79, 0.78, and 0.76, respectively [Fig. 12 (b)]. These slopes are also listed in Table 7, and reveal that as the vacuum pressure increased, the migration coefficient

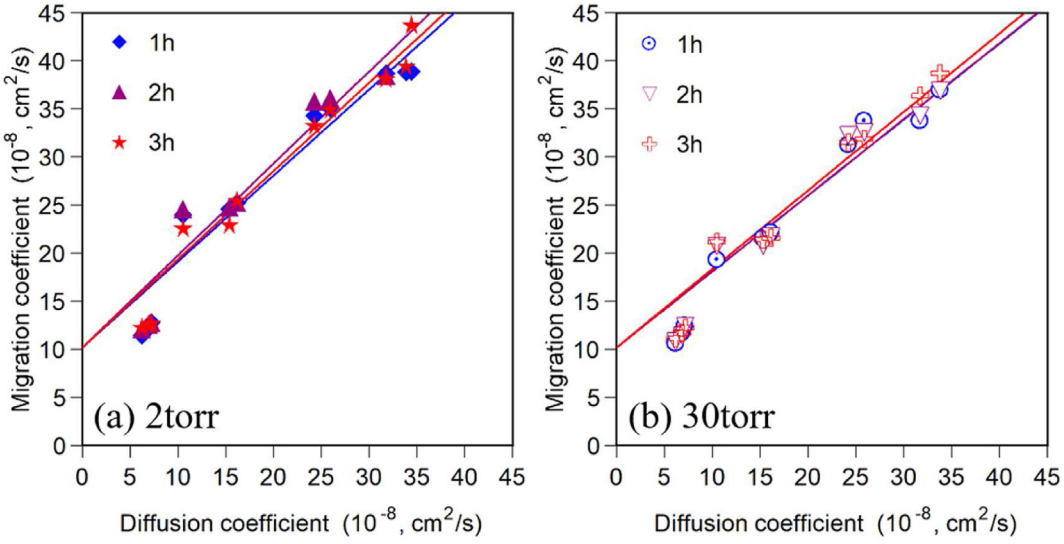

Fig. 13. The relationship between migration coefficient and diffusion coefficient in the pump-down time group: (a) 2 torr; (b)30 torr.

Table 7. The slope of migration coefficient and diffusion coefficient with various vacuum pressure.

vacuum pressure (torr)	1	2	3	7.5	15	30	45
slope (a)	0.96	0.92	0.84	0.83	0.79	0.78	0.76
R^2	0.93	0.95	0.90	0.91	0.89	0.94	0.89

Note: The R^2 is the coefficient of determination.

Table 8. The slope of migration coefficient and diffusion coefficient with various pump-down time.

pump-down time (h)	1	2	3	SD
2 torr	0.90 (0.93)	0.95 (0.92)	0.92 (0.96)	0.02
30 torr	0.79 (0.95)	0.79 (0.94)	0.82 (0.96)	0.01

Note: The value in parenthesis is the coefficient of determination; the SD is the standard deviation.

decreased more for specimens with a high diffusion coefficient than for those with a low diffusion coefficient. Accordingly, the slope decreased as the vacuum pressure increased; the slope for 1 torr was the steepest. The slopes for 1 and 2 torr were similar, with only a difference of 0.04; however, the difference between the slopes for 2 torr and 3 torr was much larger at 0.08. At 3 torr, the migration coefficient for specimens with a high diffusion coefficient decreased drastically, indicating that the degree of saturation of specimens with a high water−cement ratio decreased considerably for this pressure. Thus, the optimal vacuum pressure was determined to be 1−2 torr.

To determine the influence of migration coefficient with different pump-down time, this study controlled two vacuum pressures: 2 torr (lower than NT Build 492 specification) and 30 torr (conform to NT Build 492 specification). Fig. 13 (a) and (b) present the relationships between the migration and diffusion coefficients for different pump-down time groups with vacuum pressures of 2 torr and 30 torr; the slopes are listed in Table 8. For 2 torr, the slopes were 0.90, 0.95, and 0.92; for 30 torr, the slopes were 0.79, 0.79, and 0.82. The standard deviation of these slopes for 2 torr and 30 torr were 0.02 and 0.01, respectively. Thus, pump-down time did not significantly affect the slope of the relationship between the migration and diffusion coefficients and therefore does not affect the RCM test. This study indicates that 1−2 torr of vacuum pressure and 1 hour of pump-down time are the optimal conditions for maximizing the accuracy and efficiency of the RCM test.

4. Conclusions

According the results of experiment, the following conclusions can be drawn:

1. For RCM test with vacuum pressure group, as the vacuum pressure increased, the migration coefficient was decreased less in specimens with higher a water−cement ratio. Furthermore, the relationship between vacuum pressure and the migration coefficient approximates an exponential function. The migration coefficient decreased as the increase in vacuum pressure. Moreover, for the migration coefficient in various vacuum pressures approximated or deviated from the fitting curve, the vacuum pressure should be lower than 7.5 torr to obtain accurate results from RCM test.
2. No matter the pump-down time is 1, 2 or 3 hours, the migration coefficients was approximated with each other for specimen of C3, C4, C5, C6 with vacuum pressure 2 torr. For a vacuum pressure of 30 torr, pump-down time changes did not affect the migration coefficient of specimens with a low water−cement ratio (C3, C4), but had a greater effect for specimens with a high water−cement ratio (C5, C6). That result could be applicable by CV analysis. Accordingly, using a vacuum pressure of 2 torr can shorten the pump-down time to 1 hour and improve the test efficiency; vacuum pressures of 30 torr should not be used.
3. This research used linear regression to establish relationships between the diffusion and migration, and determined the most suitable vacuum condition by the slope of linear equation. The results indicate that 1−2 torr of vacuum pressure and 1 hour of pump-down time are the optimal conditions for maximizing the accuracy and efficiency of the RCM test.

Conflicts of interest

The authors have no conflicts of interest to report.

Acknowledgments

This research was supported by the Ministry of Science and Technology,Taiwan (MOST 109-2813-C-019-009-E and MOST 110-2221-E-019), sincere thanks.

References

[1] AASHTO T259. Standard method of test for resistance of concrete to chloride ion penetration includes all amendments and changes through reapproval notice. American association of state highway and transportation officials; 2017.
[2] AASHTO T260. Sampling and testing for chloride ion in concrete and concrete raw materials. American association of state highway and transportation officials; 2005.

[3] AASHTO T357. Predicting chloride penetration of hydraulic cement concrete by the rapid migration procedure. American association of state highway and transportation officials; 2019.
[4] Aitcin PC, Neville A. High performance concrete demystified. ACI J: Concr Int 1993;15(1).
[5] Baroghel-Bouny V, Wang X, Thiery M, Saillio M, Barberon F. Prediction of chloride binding isotherms of cementitious materials by analytical model or numerical inverse analysis. Cement Concr Res 2012;42(9):1207−24.
[6] Cao C, Cheung MMS, Chan BYB. Modelling of interaction between corrosion-induced concrete cover crack and steel corrosion rate. Corrosion Sci 2013;69:97−109.
[7] Chiang CT. Activation energy of electrical conductivity by the rapid chloride permeability test of concrete. National Taiwan Ocean University, Institute of Materials Engineering College of Engineering PhD thesis; 2009.
[8] Collepardi M, Marcialis A, Turrizuani R. Kinetics of Penetration of Chloride Ions into the concrete. II Cemento 1970;4:157−64.
[9] Crank J. The mathematics of diffusion. 1979.
[10] Halamickova P, Detwiler RJ, Bentz DP, Garboczi EJ. Water permeability and chloride ion diffusion in Portland cement mortars: relationship to sand content and critical pore diameter. Cement Concr Res 1995;29(8):790−802.
[11] Huang KS, Yang CC. Using RCPT determine the migration coefficient to assess the durability of concrete. Construct Build Mater 2018;167:822−30.
[12] Cabrera JG. Deterioration of concrete due to reinforcement steel corrosion. Cement Concr Compos 1996;18:47−59.
[13] Jin H, Li Z, Zhang W, Liu J, Xie R, Tang L, et al. Iodide and chloride ions diffusivity, pore characterization and microstructures of concrete incorporating ground granulated blast furnace slag. J Mater Res Technol 2022;16:302−21.
[14] Liu J, Wang X, Qiu Q, Ou G, Xing F. Understanding the effect of curing age on the chloride resistance of fly ash blended concrete by rapid chloride migration test. Mater Chem Phys 2017;196:315−23.
[15] Martín-Pérez B, Zibara H, Hooton RD, Thomas MDA. A study of the effect of chloride binding on service life predictions. Cement Concr Res 2000;30(8):1215−23.
[16] Naito C, Fox J, Bocchini P, Khazaali M. Chloride migration characteristics and reliability of reinforced concrete highway structures in Pennsylvania. Construct Build Mater 2020;231: 117045.
[17] NT Build 492. Chloride migration coefficient from non-steady-state migration experiments. Nordtest method; 1999.
[18] Otsuki N, Nagataki S, Nakashita K. Evaluation of the AgNO3 solution spray method for measurement of chloride penetration into hardened cementitious matrix materials. Construct Build Mater 1993;7(4):195−201.
[19] Rossi E, Roy R, Copuroglu O, Jonkers HM. Influence of self-healing induced by polylactic-acid and alkanoates-derivates precursors on transport properties and chloride penetration resistance of sound and cracked mortar specimens. Construct Build Mater 2022;319:126081.
[20] Shiu RW, Yang CC. Evaluation of migration characteristics of OPC and slag concrete from the rapid chloride migration test. J Mar Sci Technol 2020;28:69−79.
[21] Slater JE. Corrosion of metals in association with concrete. American Society for Testing Materials; 1983.
[22] Spiesz P, Brouwers HJH. Influence of the applied voltage on the Rapid Chloride Migration (RCM) test. Cement Concr Res 2012;42(8):1072−82.
[23] Tang L. Concentration dependence of diffusion and migration of chloride ions. Cement Concr Res 1999;29: 1463−8.
[24] Williamson J, Isgor OB. The effect of simulated concrete pore solution composition and chlorides on the electronic properties of passive films on carbon steel rebar. Corrosion Sci 2016;106:82−95.
[25] Yang CC, Tsai YM, Yang KC. The Relationship between Migration Time in ACMT and Ponding Time in Ponding Test for Cementitious Materials. J Mar Sci Technol 2012;20(2): 281−9.